



On near-source earthquake triggering

Tom Parsons¹ and Aaron A. Velasco²

Received 29 December 2008; revised 28 June 2009; accepted 9 July 2009; published 3 October 2009.

[1] When one earthquake triggers others nearby, what connects them? Two processes are observed: static stress change from fault offset and dynamic stress changes from passing seismic waves. In the near-source region ($r \leq 50$ km for $M \sim 5$ sources) both processes may be operating, and since both mechanisms are expected to raise earthquake rates, it is difficult to isolate them. We thus compare explosions with earthquakes because only earthquakes cause significant static stress changes. We find that large explosions at the Nevada Test Site do not trigger earthquakes at rates comparable to similar magnitude earthquakes. Surface waves are associated with regional and long-range dynamic triggering, but we note that surface waves with low enough frequency to penetrate to depths where most aftershocks of the 1992 $M = 5.7$ Little Skull Mountain main shock occurred (~ 12 km) would not have developed significant amplitude within a 50-km radius. We therefore focus on the best candidate phases to cause local dynamic triggering, direct waves that pass through observed near-source aftershock clusters. We examine these phases, which arrived at the nearest (200–270 km) broadband station before the surface wave train and could thus be isolated for study. Direct comparison of spectral amplitudes of presurface wave arrivals shows that $M \sim 5$ explosions and earthquakes deliver the same peak dynamic stresses into the near-source crust. We conclude that a static stress change model can readily explain observed aftershock patterns, whereas it is difficult to attribute near-source triggering to a dynamic process because of the dearth of aftershocks near large explosions.

Citation: Parsons, T., and A. A. Velasco (2009), On near-source earthquake triggering, *J. Geophys. Res.*, 114, B10307, doi:10.1029/2008JB006277.

1. Introduction

[2] Foreshocks, main shocks, aftershocks, doublets, or triggered earthquakes are some of the names given to earthquakes linked in time and space. Whatever they are called, earthquakes clearly respond to interactive stressing through the Earth's crust [Freed, 2005]. Understanding how one earthquake leads to another is important for seismic hazard forecasting. Two explanations for earthquake triggering have emerged; one view has earthquake slip and resulting crustal offset causing a lasting, static stress change that triggers subsequent events [Yamashina, 1978; Das and Scholz, 1981; Stein and Lisowski, 1983; King et al., 1994; Stein, 1999]. An alternative hypothesis posits triggering mostly from dynamic stress changes generated by seismic waves [Cotton and Coutant, 1997; Belardinelli et al., 1999; Kilb et al., 2000; Gomberg et al., 2003; Felzer and Brodsky, 2006]. In the near-source region, a complex mixture of the two triggering modes may initiate the same physical process in terms of aftershock nucleation [Kilb et al., 2002; Voisin et al., 2004].

[3] At great distances from a source event, static stress changes become infinitesimally small, leaving little doubt

that observed earthquake rate increases are prompted by dynamic stress changes from passing seismic waves [Hill et al., 1993; Gomberg et al., 2004; Hill, 2008; Velasco et al., 2008], although the underlying physics behind dynamic triggering remains to be explained and is likely complicated by secondary triggering [Ziv and Rubin, 2003; Ziv, 2006]. Given the temporal correlations between distant earthquake rate increases with passing seismic waves, it is reasonable to suggest that a significant fraction of near-source (1–5 main shock rupture lengths) aftershocks are dynamically triggered as well. We focus on the near-source region because it is where hazard forecasters are most concerned about how to address the stress legacy from past earthquakes [e.g., Working Group on California Earthquake Probabilities, 2003].

[4] Balancing triggering modes in the near-source region has been a difficult problem to solve because the primary data signal is the observation of seismicity rate increases that are temporally and spatially correlated with the occurrence of moderate-to-large earthquakes. Rate increases typically occur where few events were happening before the triggering event. Once an initial main shock happens, multiple triggering sources may begin a cascade of static and/or dynamic stress changes [e.g., Felzer et al., 2003]. Thus, it is relatively easy to make correlations, but very difficult to establish causation.

¹U.S. Geological Survey, Menlo Park, California, USA.

²Department of Geological Sciences, University of Texas at El Paso, El Paso, Texas, USA.

[5] In this paper, we gain insight into earthquake triggering by comparing effects of earthquakes and large explosion sources. Different triggering sources deliver different dynamic and static stresses into the surrounding crust at the Nevada Test Site where we conducted our analysis [e.g., *Walter et al.*, 1995]. We work with California and Nevada earthquake catalogs (source Advanced National Seismic System (ANSS) composite catalog) from mid-1992, when there were large and moderate earthquakes (28 June 1992 $M = 7.4$ Landers, and 29 June 1992 $M = 5.7$ Little Skull Mountain) coincident with large explosions ($M \leq 5.5$) detonated at the Nevada Test Site. Our goal is to examine seismicity rate changes from earthquake and explosive sources and exploit differences in the dynamic and static stresses they cause in order to explain near-source earthquake triggering.

2. Observations of Triggering by Earthquakes and Nuclear Explosions Near the Nevada Test Site

[6] We focus on a seismically active region that has moderate earthquakes and large explosions in close temporal and spatial proximity. We examine catalog and waveform data from the Nevada Test Site from 1991 to 1992 when there were several test blasts up to $M = 5.5$, and when the $M = 7.4$ Landers and $M = 5.7$ Little Skull Mountain earthquakes occurred. We compare regional seismicity rates before and after moderate local earthquake, nuclear explosions, and distant large earthquake sources to establish their relative triggering characteristics (Figure 1 and Table 1).

2.1. Issues of Catalog Completeness and Rate Change Significance

[7] We examine rates of $M \leq 3$ earthquakes from California and Nevada earthquake catalogs (ANSS composite catalog) because most of the triggering source earthquakes that we use are between $M = 3$ and $M = 5$ (Table 1). We estimate, using the goodness of fit method of *Wiemer and Wyss* [2002], that the regional ANSS catalog is complete above $M = 2$ during the 1992 period of interest (Figure 2).

[8] Our rate change observations are also subject to concerns about varying event detection thresholds both temporally and spatially. This might be mitigated somewhat in that our rate change calculations are conducted within limited geographic regions and cover periods of days or hours. Many worthwhile observations can be made about the earliest initiation of seismic activity at different localities during the hours between the 28 June 1992 $M = 7.4$ Landers, and 29 June 1992 $M = 5.7$ Little Skull Mountain earthquakes. This period is subject to significant catalog detection issues [e.g., *Kagan*, 2004], but any events that initiated in clusters in the 22 h prior to the Little Skull Mountain shock are useful regardless of short-term detection thresholds because they demonstrate activity that cannot be associated with that $M = 5.7$ event. We thus study all catalog events above the overall completeness level ($M \geq 2$), but conduct significance testing on rate change calculations.

[9] In this paper, we show plots of raw data as the occurrences of earthquakes over time, and we also show calculated rate changes (Figure 1). Generalized methods exist for testing the significance of seismicity rate change observations [e.g., *Habermann*, 1987; *Matthews and Reasenberg*, 1988; *Marsan and Nalbant*, 2005]; however because we

stack events from multiple sources (process described in section 2.2.) we must determine rate change significance by repeatedly sampling variability of the background seismicity using the same process that we apply to calculating rate changes.

[10] To test significance of calculated rate changes, we use the locations of triggering sources, but we randomize their times across the periods of interest (Julian day 181 to 311 in 1992). For example, the earthquake trigger source events identified as stars in Figure 1 are each given 100 different randomly assigned origin times across the 1992 period they occurred. The mean daily rate variations within the 250-km range of the source events and confidence intervals associated with those 100 times are calculated. In this way we capture some of the inherent rate variability and potential varying detection threshold effects in the catalog, and can assess whether a calculated rate change is significant. We also calculate the beta statistic [*Matthews and Reasenberg*, 1988] for reference.

2.2. Triggered Earthquake Rate Observations

[11] To gain a generalized view of the relative triggering ability of large explosions and comparable magnitude earthquakes, we stack $M \leq 3$ seismicity from 5 days before and after periods for eight each nuclear explosions and earthquakes. Thus, zero time in Figure 1c is the origin time of each potential triggering source, and all other earthquake times in the 5-day periods before and after each triggering source are given as relative to the sources and combined into one catalog. Event rates are generally low (particularly around the nuclear explosions) making rate changes associated with any one event difficult to quantify. However, stacking before and after periods of multiple events increases the sample and significance; the histogram and earthquake maps of Figure 1 are complicated by the stacking process in that some of the large earthquakes happened less than 5 days apart. Therefore, some of the “after” events from one source can become “before” events for the next. This type of analysis is useful because the overall elevated seismicity rates enable quantitative rate change assessments [e.g., *Toda and Stein*, 2003; *Ziv*, 2006]. We conduct this analysis over short periods because the entire region was affected by the 28 June 1992 $M = 7.4$ Landers earthquake, which caused dynamic triggering throughout the western United States and was suggested as a cause of the 29 June 1992 $M = 5.7$ Little Skull Mountain event that happened 22 h after it [*Hill et al.*, 1993; *Gomberg and Bodin*, 1994; *Anderson et al.*, 1994]. The Landers shock was also suggested as a source of significant static stress triggering, including the $M = 6.5$ Big Bear earthquake that occurred 3 h 26 min later and was associated with a 0.2–0.3 MPa static stress increase [*King et al.*, 1994].

[12] The results we see at the Nevada Test Site show large explosion sources to be poor earthquake triggers compared with comparable magnitude earthquakes (mean explosion magnitude was $M = 4.7$, mean earthquake magnitude was $M = 4.0$). Other than aftershocks related to cavity collapse, this result is generally observed in regional catalogs after nuclear tests and likely results from small tectonic stress change and shallow source depth [e.g., *Brune and Pomeroy*, 1963; *Boucher et al.*, 1969; *Hamilton et al.*, 1969; *Toksoz and Kehler*, 1972; *Adushkin and Spivak*, 1995; *Nikolaev*, 1995;

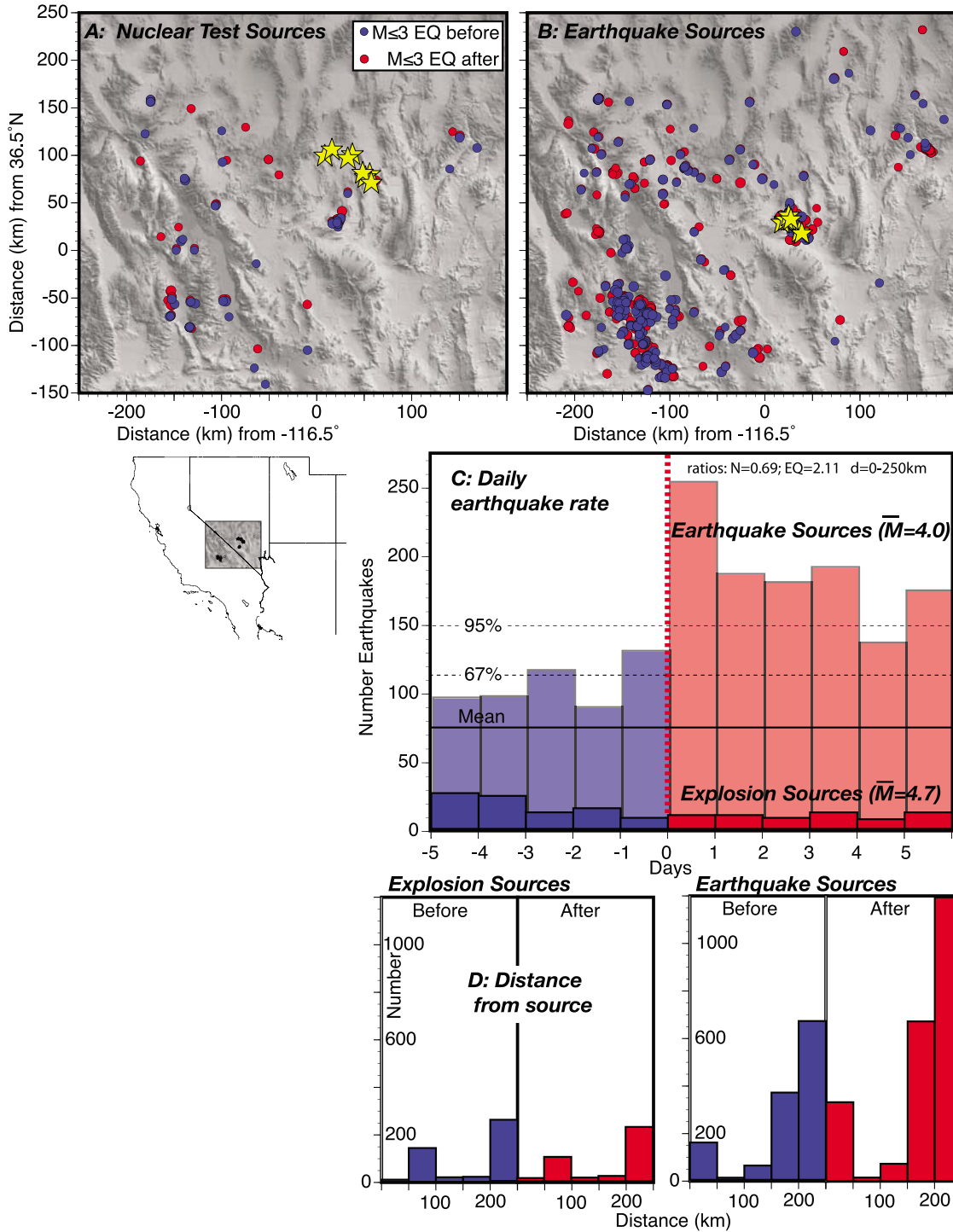


Figure 1. Comparison of relative triggering ability between similar magnitude nuclear explosions and earthquakes at the Nevada Test Site. (a) Spatial distribution of $2 \leq M \leq 3$ seismicity for 5 days before (blue) and after (red) eight nuclear explosions (stars). (b) Spatial distribution of $2 \leq M \leq 3$ seismicity for 5 days before and after eight earthquakes (stars; see Table 1 for source information). (c) The number of $2 \leq M \leq 3$ earthquakes per day (relative to source origin times) within a 250-km radius before and after eight nuclear explosions (at bottom of histogram) and $M > 3$ source earthquakes are shown. Confidence intervals on background rate variations from 100 randomly sampled intervals in 1992 are shown. Explosion sources produce no discernable triggering whereas earthquakes cause a near doubling of the rate in the first days after they occur. (d) Histograms show the number of before and after events versus radial distance from sources.

Table 1. Earthquake and Nuclear Explosion at the Nevada Test Site Sources Used to Compare Relative Triggering Ability

Year	Origin Time		Location		Magnitude	Depth (km)	Name
	Julian Day	Time (UT)	Latitude	Longitude			
<i>Earthquakes</i>							
1992	181	1014:20.06	36.6378	-116.1708	5.7	13.09	Little Skull Mountain
1992	181	1031:00.88	36.6257	-116.1473	4.7	12.90	Aftershock
1992	186	0557:30.83	36.7293	-116.2975	2.8	9.72	Aftershock
1992	187	0654:13.08	36.7277	-116.2748	4.4	13.00	Aftershock
1992	257	1146:20.82	36.7243	-116.3047	4.3	9.30	Aftershock
1992	282	1223:56.87	36.7602	-116.2713	3.4	10.30	Aftershock
1992	283	0016:17.86	36.7317	-116.2505	3	9.50	Aftershock
1992	311	2024:03.78	36.7070	-116.3360	3.3	6.00	Aftershock
<i>Nuclear Explosions</i>							
1991	227	1600:00.00	37.0870	-116.0030	4.2	0.488	Floydada
1991	257	1900:00.005	37.2260	-116.4290	5.5	0.671	Hoya
1991	262	1530:00.067	37.2360	-116.1670	4	0.264	Distant_Zenith
1991	291	1912:00.00	37.0630	-116.0460	5.2	0.457	Lubbock
1991	330	1835:00.1	37.0960	-116.0700	4.6	0.457	Bristol
1992	86	1630:00.00	37.2720	-116.3610	5.5	0.64	Junction
1992	262	1700:00.078	37.2070	-116.2110	4.4	0.385	Hunters_Trophy
1992	267	1504:00.00	37.0210	-115.9890	4.4	0.426	Divider

Richards and Ekström, 1995]. The histogram from Figure 1c shows no discernable rate change associated with large explosions, whereas earthquake sources were associated with a nearly doubled rate of earthquakes within a 250-km radius in the 5 days following them compared with the preceding 5-day period. Comparison of individual earthquake and explosion events over longer periods yields the same result; Figure 3 shows seismicity for 100 days before and after the $M = 5.7$ Little Skull Mountain earthquake and the $M = 5.5$ “Hoya” nuclear explosion. The comparable magnitude nuclear blast has no discernable associated seismicity, whereas the Little Skull Mountain earthquake is correlated with a productive aftershock sequence.

[13] We see two interpretations that can be made from comparing large explosion and earthquake triggering sources: (1) static stress changes dominate in the near-source region because the rate increase is greatest there from earthquake sources, and absent from explosions, or (2) significant

triggering results from dynamic effects, but explosion sources are poor dynamic triggers because they lack enough amplitude at necessary frequencies and depths. These interpretations are examined in detail in sections 3 and 4.

3. Near-Source Static Stress Triggering Model

[14] From Figure 1 we note a significant seismicity rate increase following earthquake sources at the Nevada Test Site that occurred within 50 km of the sources. We see no such effect from comparable magnitude nuclear explosions, which cause less tectonic strain than earthquakes, although they are observed to generate some [e.g., *Brune and Pomeroy*, 1963; *Boucher et al.*, 1969; *Hamilton et al.*, 1969; *Toksoz and Kehrner*, 1972; *Adushkin and Spivak*, 1995; *Nikolaev*, 1995]. At the Nevada Test Site, aftershocks are typically $M \leq 2$ and are restricted to less than 5 explosion cavity radii from the source point; these microshocks are

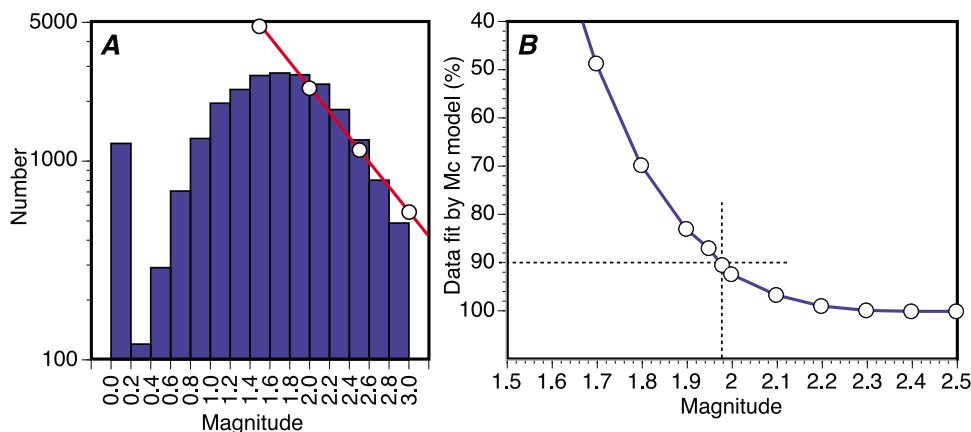


Figure 2. (a) Histogram of magnitude versus frequency in the California and Nevada ANSS composite catalog for the 1992 calendar year. The b value trend of 1.07 is plotted for reference. (b) The magnitude completeness (M_c) level is determined using the goodness of fit test of *Wiemer and Wyss* [2002], where a cutoff is defined in which a predefined percentage (90%) of the observed data is modeled by a straight line. Note that it is not the minimum percentage that is chosen. A 95% level of fit is rarely obtained for real catalogs; the 90% level is a compromise value [*Woessner and Wiemer*, 2005].

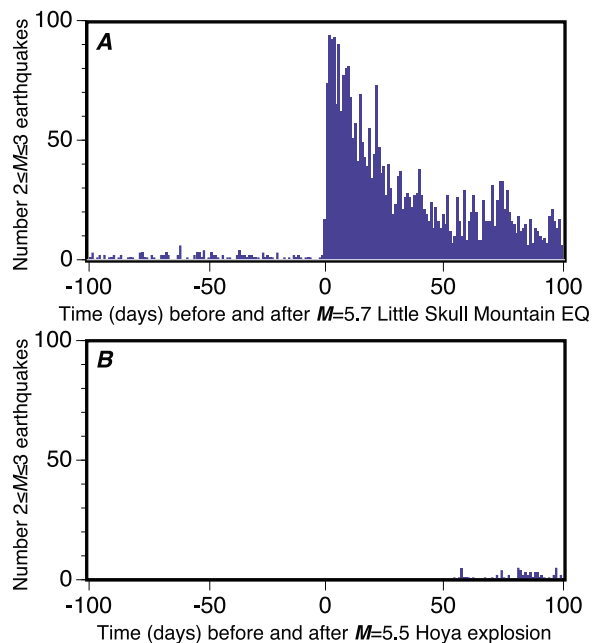


Figure 3. Comparison of seismicity rates within 250 km of and 100 days before and after (a) the $M = 5.7$ Little Skull Mountain earthquake and (b) the $M = 5.5$ “Hoya” nuclear explosion. While triggered seismicity and an Omori law rate decay are obvious after the Little Skull Mountain event, aftershocks are completely absent following the nuclear explosion.

associated with cavity collapse [e.g., Richards and Ekström, 1995] and do not appear in the ANSS catalogs.

[15] Earthquakes did commonly occur in 1992 throughout the test site region, including very close to sites of large nuclear explosions. Thus, the lack of near-source earthquake rate increases following nuclear explosions is not because of low ambient stress or a dearth of earthquake faults. One hypothesis we examine is that near-source triggering results from static stress triggering through Coulomb stress transfer [e.g., King et al., 1994; Stein, 1999]; we expect shearing earthquake sources to generate much greater Coulomb stress changes than volume-changing explosions [Nikolaev, 1995; Richards and Ekström, 1995].

[16] To compare the expected static stress change effects from nuclear explosions with earthquakes, we model a typical cavity collapse [e.g., Houser, 1969] associated with a nuclear test (Figure 4). We use a finite element model (ANSYS© multiphysics code) with a spherical cavity centered at 0.67 km depth, which was the depth of the “Hoya” blast (Table 1) that had the closest magnitude ($M = 5.5$) as the $M = 5.7$ Little Skull Mountain earthquake during the 1991–1992 study period. We create a two-layer model, with the upper layer simulating the worked, unwelded tuff layer (Young’s modulus of $E = 9.8$ GPa [Schultz and Li, 1995]) where Pahute Mesa test blasts like Hoya were sourced [Drellack et al., 2001]. The lower layer represents a granitic substrate with a Young’s modulus of $E = 80$ GPa [Birch, 1966]. We calculate stress changes on optimally oriented planes using a friction coefficient of $\mu = 0.4$. Our calculations reinforce the conclusions of many previous observers that primary strain from nuclear blasts is spatially limited to

within a few radii of the cavity (Figure 4) [e.g., Brune and Pomeroy, 1963; Boucher et al., 1969; Hamilton et al., 1969; Toksoz and Kehrner, 1972; Adushkin and Spivak, 1995; Nikolaev, 1995]. We show that Coulomb stress changes in excess of 0.01 MPa (minimum threshold commonly associated with static stress triggering [e.g., Reasenber and Simpson, 1992; Hardebeck et al., 1998; Harris, 1998]) are limited to within a ~ 5 -km radius hemisphere surrounding the cavity (Figure 4). Our calculations represent a maximum stress change because the model layers are perfectly elastic and thus do not account for stress losses from fracturing, compaction, and high-temperature inelastic deformation within the collapsing cavity.

[17] We also calculate Coulomb stress changes from the $M = 5.7$ Little Skull Mountain event to investigate the likely reach of earthquake-generated static stress transfer (Figure 4). Multiple estimates of Little Skull Mountain rupture characteristics are found in the literature; we model two versions but find little difference at the scale we are investigating. Meremonte et al. [1995] reported that the strike of 55° , dip of 56° SE, with rake of -71° ; we combine this model with the moment estimate of 9.8×10^{17} N m given by Walter [1993]. We also apply the model given by Lohman et al. [2002], who suggested that the strike of 36° , dip of 58° SE, rake of -76° , and a 3.2×10^{17} N m moment. Both models show a maximum static Coulomb stress change reach of about 30 km from the source if the 0.01 MPa minimum threshold is applied (Figure 4c). We calculate stress changes on optimally oriented planes using a friction coefficient of $\mu = 0.4$ in the same manner as with the nuclear cavity collapse model. The comparison demonstrates that shearing earthquake sources generate Coulomb stress changes that extend much farther from the source than large explosions of comparable magnitude, which is consistent with seismicity observations.

[18] While the 29 June 1992 $M = 5.7$ Little Skull Mountain event occurred within a period of generally elevated seismic activity caused by the 28 June 1992 $M = 7.4$ Landers earthquake [Hill et al., 1993; Gomberg and Bodin, 1994; Anderson et al., 1994], it had a secondary effect on local earthquake rates that is clearly demonstrated by Figures 5 and 6. During the 24-h period before the Little Skull Mountain shock seismic activity was limited mainly to the Coso volcanic center in eastern California (Figure 5a). Within 24 h after Little Skull Mountain earthquake, $M \leq 3$ seismicity rates increased in the vicinity of the main shock and at the Coso site ~ 150 km southwest of the main shock (Figure 5b). This could have been evolution of seismic clusters begun by dynamic triggering from Landers, or enhancement from the Little Skull Mountain shock. The Little Skull Mountain cluster has different initiation characteristics than others attributed to the Landers shock (Figure 6), showing an Omori law temporal decay pattern.

[19] Given that the Little Skull Mountain earthquake occurred in the aftermath of the Landers shock, it will always be difficult to attribute unequivocal causation of seismicity rate changes at the Nevada Test site to local events. However, the sharp rise in seismicity rate clustered at the immediate vicinity of, and that began just after the Little Skull Mountain earthquake is most likely triggered locally. We demonstrate that the cluster correlates spatially with the extent of calculated static Coulomb stress change (Figures 4 and 5). We

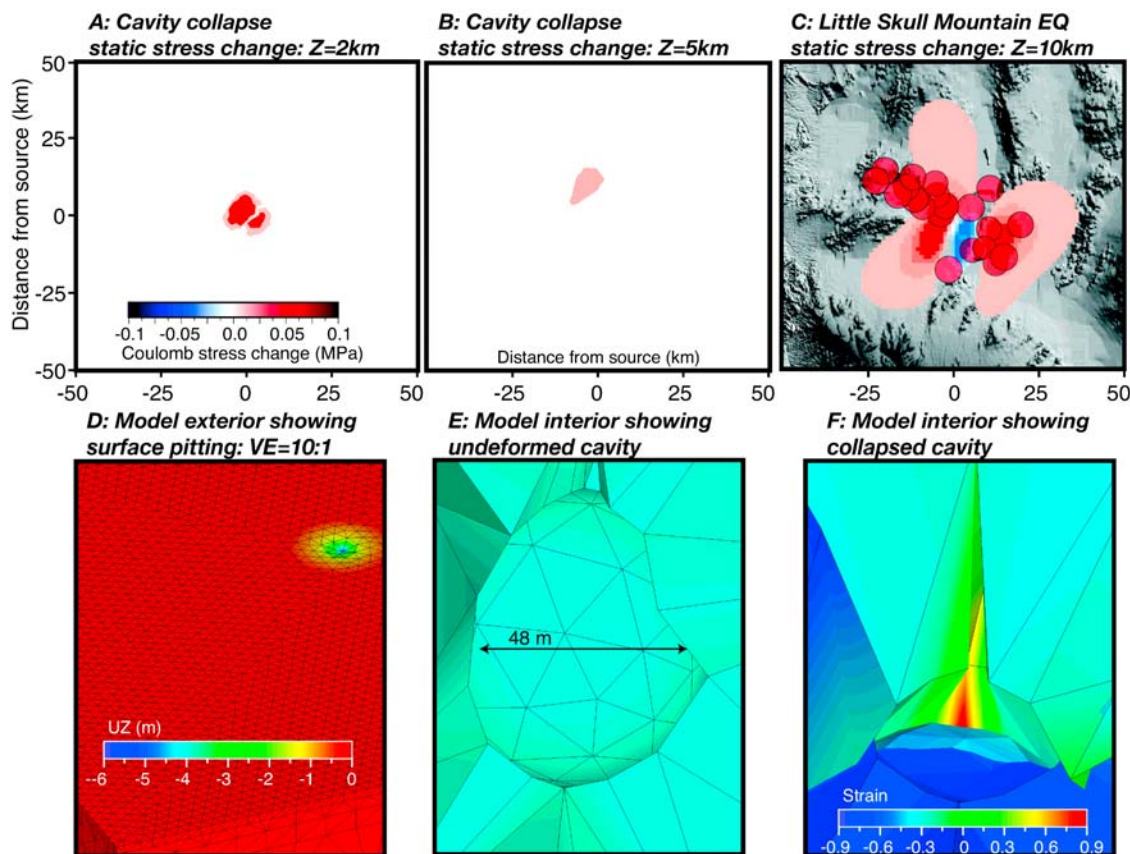


Figure 4. Comparison of modeled Coulomb stress from cavity collapse associated with nuclear explosion at (a) 2 km depth and (b) 5 km depth with (c) stress change modeled for the Little Skull Mountain earthquake at 10 km depth (increases greater than 0.01 MPa shown in red, decreases less than -0.01 MPa are shown in blue). Calculated stress change from cavity collapse was less than threshold value of 0.01 MPa at 10 km depth. (d) The exterior of the finite element model is shown including surface pitting from cavity collapse. (e) A close-up view of the undeformed spherical cavity which was 48 m wide, and (f) the collapsed cavity is shown as contoured with local strain values.

further note a gap in seismic activity/rate increase beyond the static stress change threshold at about 50 km from the epicenter, which is evident on the map of Figure 5b.

[20] In summary, we conclude that near-source earthquake triggering can be attributed to a static stress change model because (1) the calculated spatial extent of static Coulomb stress change of the Little Skull Mountain earthquake is correlated with the distribution of near-source aftershocks (Figure 4c) and (2) large explosions of equivalent magnitude fail to produce triggered earthquakes, which can be explained by the limited (~ 5 km) spatial reach of Coulomb stress changes they appear to generate (Figures 4a and 4b).

4. Near-Source Dynamic Triggering Model

[21] The primary data signal we observe at the Nevada Test Site is seismicity rate increases following main shock earthquakes. The Little Skull Mountain cluster is an example that can be explained with a near-source (within 50 km) static stress-triggering model. However, the absence of any activity prior to the Little Skull Mountain shock means that no rate decrease can be calculated and thus no diagnostic [e.g., Felzer and Brodsky, 2005; Mallman and Parsons, 2008]

stress shadowing [Harris and Simpson, 1996] can be shown (correlated seismicity rate and stress decreases). Therefore, an overall rate increase might also be attributable to dynamic stresses caused by seismic waves radiating out from the source event.

[22] Our goal is to assess whether near-source triggering occurs through a static or dynamic process, but we begin our dynamic triggering analysis in the far field, where static triggering cannot be the cause, in order to establish whether dynamic triggering can be shown at any range. We therefore show details of the relative timing of seismicity rate fluctuations at the Coso site in relation to the origin times of the Landers and Little Skull Mountain events in Figure 5c. Seismicity rates did not rise immediately as seismic waves from either earthquake passed through the Coso site, but rose gradually, peaking about 12 h after the Landers shock, and again about 16 h after the Little Skull Mountain earthquake (Figure 5c). If the 22-h periods before and after the Little Skull Mountain events are compared at Coso, the seismicity rate increase is highly significant (exceeding 99% confidence using the beta statistic [Matthews and Reasenberg, 1988]). However, given the delayed onset of dynamically triggered events at other localities (Figures 6a and 6b) from the

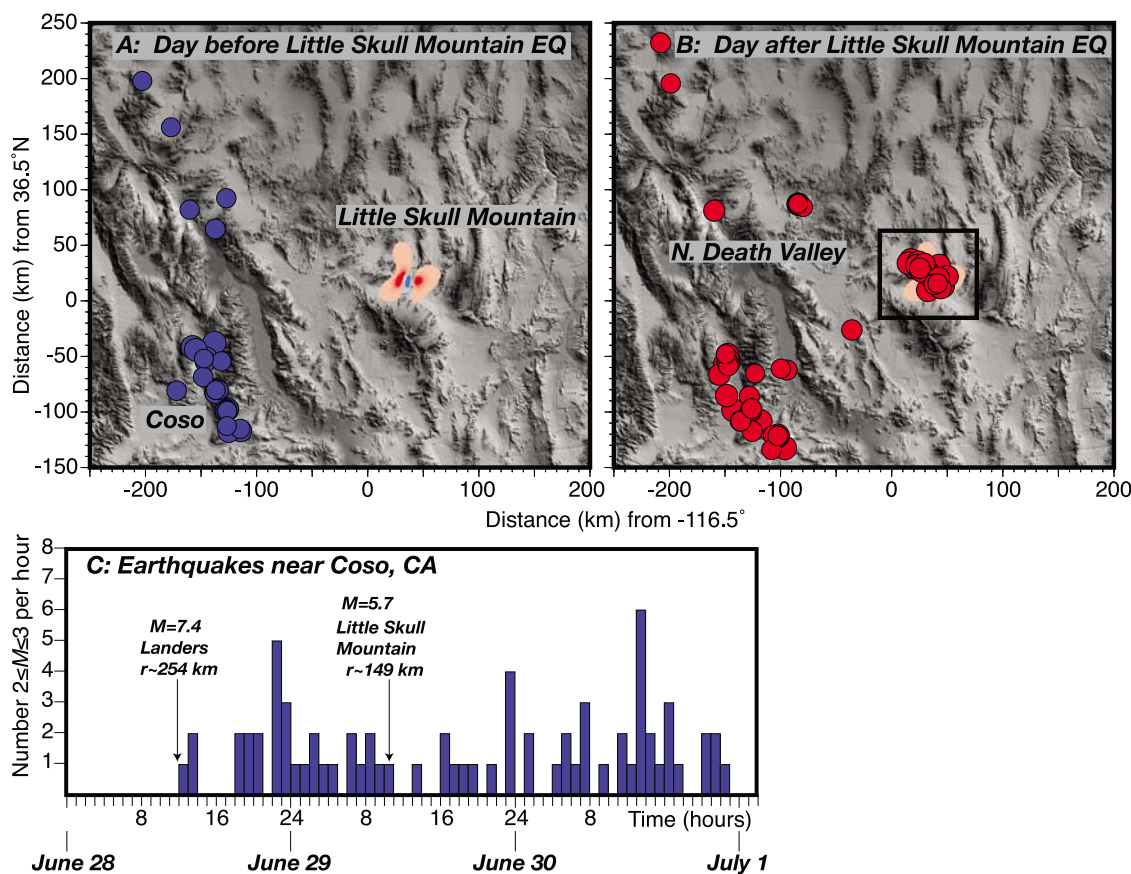


Figure 5. (a) Map of $2 \leq M \leq 3$ earthquake distribution 24 h prior to the $M = 5.7$ Little Skull Mountain earthquake in 1992. Earthquake activity was restricted to the Coso volcanic region of California. The calculated static stress change from the Little Skull Mountain event is shown. (b) The day after the Little Skull Mountain event shows activity both near the epicenter as well as at remote locations, including the Coso site, although from the time series shown in Figure 5c, it is clear that Coso earthquake rates rose in the hours after the $M = 7.4$ Landers earthquake, likely the result of dynamic triggering from the source ~ 250 km away (boxed area corresponds to the stress change image shown in Figure 4c). (c) Earthquakes near Coso.

Landers earthquake, seismicity rate increases at Coso could be due to the Landers event rather than the Little Skull Mountain shock.

[23] If we do interpret the secondary rate increase at Coso as dynamic triggering from the Little Skull Mountain earthquake, then it is reasonable to suggest that some fraction of the near-source cluster was also dynamically triggered. To investigate this hypothesis, we compare the dynamic signal from earthquakes and nuclear explosions. The purpose for this comparison is twofold: (1) if there are significant differences in dynamic stresses between nuclear and earthquake triggers, then we can identify which phases/frequencies are potentially responsible for near-source dynamic triggering; and (2) alternatively, if the two sources deliver the same near-source dynamic stresses into the crust, then we can conclude that the static stress change is the primary cause of near-source triggering since explosions do not cause significant static stress changes.

4.1. Modeled Amplitude Versus Depth and Frequency of Surface Waves

[24] We begin our comparison of earthquake and nuclear triggering by examining the potential role of surface wave

triggering in the near-source region, since surface waves are well established triggers at regional and teleseismic distances [e.g., Hill *et al.*, 1993; Gomberg *et al.*, 2004; Hill, 2008; Velasco *et al.*, 2008].

[25] Generally, earthquake and nuclear explosions differ in the excitation of surface waves and P waves [e.g., Stevens and Day, 1985]. The differences are caused by source spectral characteristics, source region elastic properties (explosions occur shallower and in lower-velocity material), and focal mechanisms (double couple for earthquakes versus compressional sources) [e.g., Stevens and Day, 1985]. In fact, these differences explain the effectiveness of the body wave magnitude (m_b) versus surface wave (M_s) discriminant. In general, explosions will show higher m_b than M_s ; thus plotting m_b versus M_s can reveal nuclear explosions. We thus use M_s to compare magnitudes of earthquakes and nuclear explosions, which we report in Table 1.

[26] To address the differences between nuclear explosion and earthquake excitation, Gomberg and Bodin [1994] computed strains at different receiver depths using a velocity model appropriate for the Landers region to calculate surface wave amplitude as a function of depth for nuclear explosions. Moreover, they addressed the fact that triggering does not

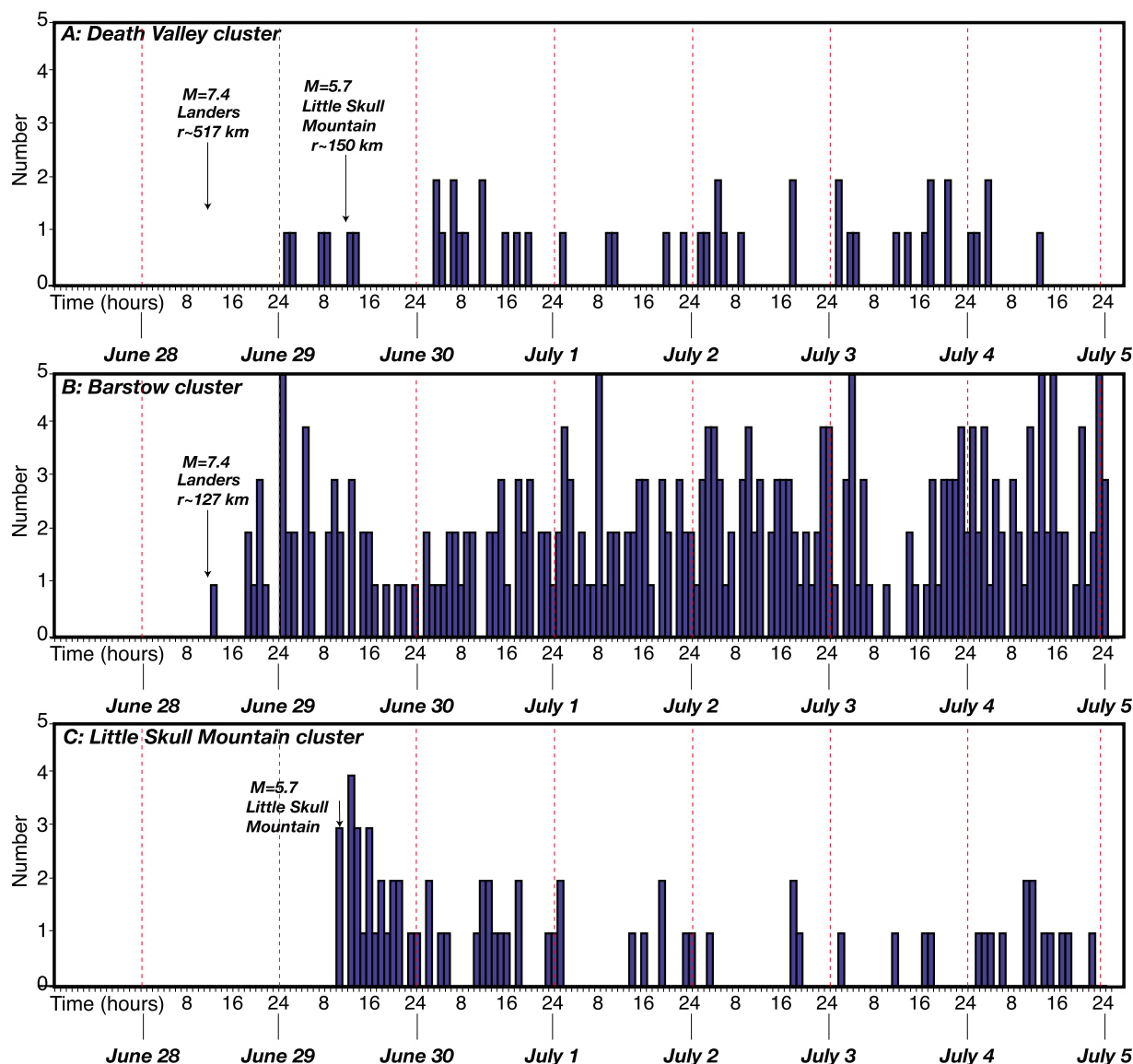


Figure 6. Time series of June–July 1992 earthquake occurrence in clusters at (a) Death Valley, (b) Barstow, California and (c) Little Skull Mountain. As at the Coso site depicted in Figure 4, remotely triggered clusters at Death Valley and Barstow show delays of 6–12 h after dynamic waves passed through the sires. In contrast, seismicity rates adjacent to the Little Skull Mountain site peaked with the main shock and decayed more like an Omori law sequence.

appear to have occurred historically for the numerous nuclear tests with local magnitude ~ 5 . From strain modeling of shallow (0.3 km) nuclear explosions, they show that amplitudes fall off as a function of depth (from ~ 3 at the surface to ~ 0.03 strain for ε_{zz} at 10 km) for a frequency range between 0.01 and 5 Hz. They thus concluded that nuclear explosions would not have significant ability to trigger earthquakes at depth.

[27] For surface wave triggering from either nuclear or earthquake sources, we wish to further investigate this result. It is common to calculate surface wave amplitude versus depth using eigenfunctions, which give the displacement and stresses for fundamental or higher-mode surface waves [e.g., *Aki and Richards*, 1980]. We compute eigenfunctions for a range of frequencies using the approach of *Herrmann and Ammon* [2002] for fundamental mode surface waves.

We plot vertical and radial displacements as a function of depth for 0.2 and 0.05 Hz waves, and for two velocity models (Figure 7), the Landers model chosen by *Gomberg and Bodin* [1994], and a model developed for the Little Skull Mountain region [*Smith et al.*, 2001]. Like *Gomberg and Bodin* [1994], we show that 0.2 Hz surface waves do not penetrate to depths appropriate to trigger aftershocks like those around the Little Skull Mountain event (majority at ~ 12 km). However, lower-frequency (0.05 Hz) surface waves will not lose any of their vertical component amplitudes at 12 km depth. Thus, longer period surface waves would likely be responsible for triggering events at depth.

[28] So far we have shown that regardless of the source, the most likely surface waves to be present at the depth where most aftershocks were observed near the Little Skull Mountain earthquake were those with the lowest frequency

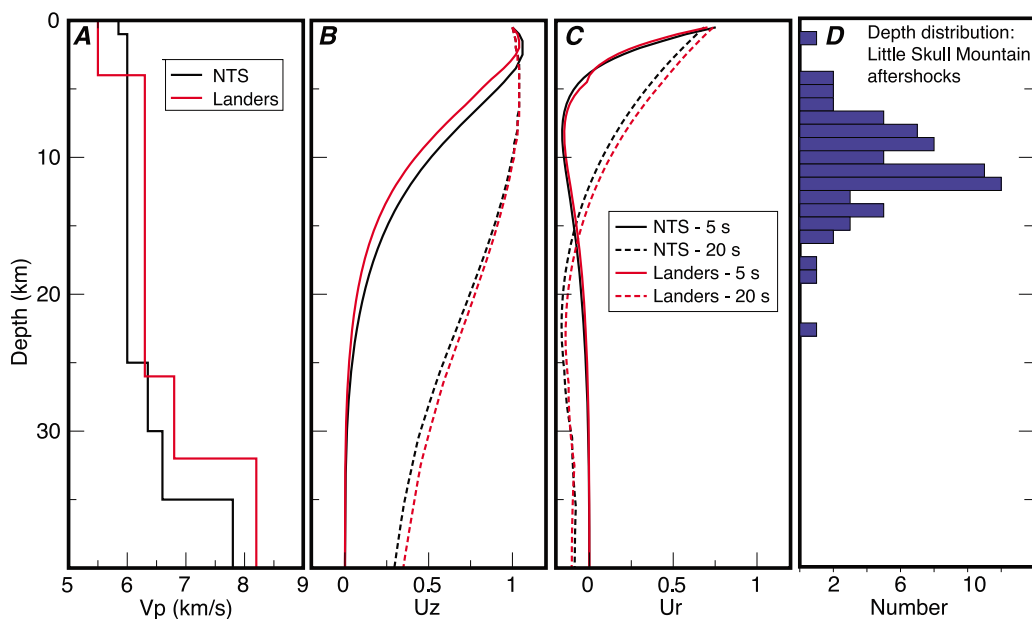


Figure 7. Velocity models and fundamental mode eigenfunctions computed for 5 s and 20 s plotted as a function of depth. Model NTS is from *Smith et al.* [2001], and the Landers model is from *Campillo and Archuleta* [1993]. Note the greatest amplitude fluctuations occur as function of period, not choice in velocity model. Thus, it is unlikely that a 5 s surface wave will trigger a tectonic event at depth.

(0.05 Hz). Higher-frequency waves (0.2 Hz) are mostly trapped within the upper 5 km of crust where relatively few aftershocks are observed (Figure 7d). However, for the near-source region there is an additional aspect of surface wave generation to take into account. Low-frequency surface waves require offset from their source before they can form out of a whole or midcrustal waveguide [e.g., *Savarensky et al.*, 1970; *Fu*, 2006]. If observed low-frequency (0.33 Hz) Rayleigh wave amplitudes are plotted as function of source distance (Figure 8) [*Karnik*, 1962], it is clear that they have orders of magnitude lower amplitudes at sub-100-km distances from sources. We replicate this general result for the Little Skull Mountain earthquake by using the reflectivity method of *Kennett* [1983], as implemented by *Randall et al.* [1995], and the source parameters/velocity model of *Smith et al.* [2001] to fit observations at the nearest (200 km) broadband station (GSC), and we extrapolate back to the source. A low-passed (≤ 0.2 Hz) record section of seismograms versus distance is presented in Figure 9, which shows the amplitude onset of sub-0.2 Hz precritical trapped surface waves to be at about 75–80 km from the source, consistent with models by *Fu* [2006]. Thus, based on direct observation and modeling results, dynamic triggering would have to be attributable to direct/reflected *P* or *S* waves impinging into the crust (Figure 10) rather than surface waves in the near-source region (0–50 km).

4.2. Observed Spectral Differences Between Earthquakes and Nuclear Sources

[29] Dynamic earthquake triggering is most clearly observed in the far field, and correlates with the passage of surface waves [e.g., *Hill et al.*, 1993; *Gomberg et al.*, 2004; *Hill*, 2008; *Velasco et al.*, 2008]. However, as described in section 4.1, higher-frequency surface waves tend to be trapped close to the surface, above where most aftershocks

are observed near the Little Skull Mountain earthquake (Figure 7), while deeper-penetrating lower-frequency surface waves have little amplitude in the near-source region

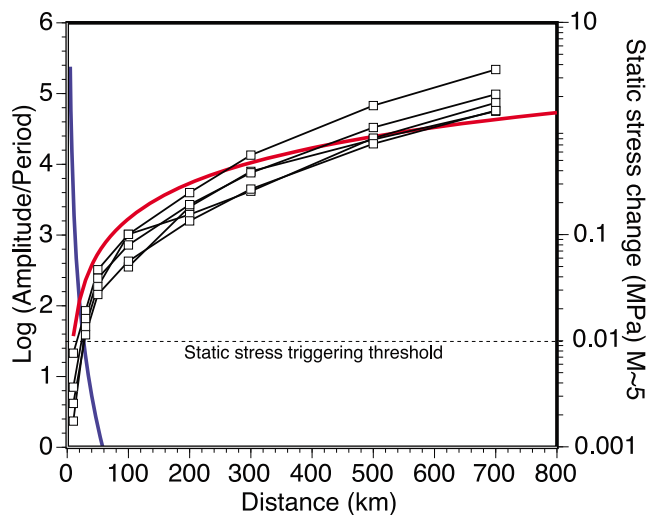


Figure 8. Ground amplitude divided by period versus distance of Rayleigh waves (data points for frequencies $f \leq 0.33$ Hz), taken from the database of *Karnik* [1962], who developed the “Prague formula” used to calculate surface wave magnitudes (plotted as red line; intended for frequencies $f \geq 0.25$ Hz). The observation is that lower-frequency surface waves have low amplitudes at sub-100-km distances from sources. Thus, the triggered seismicity in the nearest 50 km from the Little Skull Mountain earthquake (Figures 4 and 5) might best be ascribed to static stress triggering rather than dynamic stresses. Blue line shows decay of static stress change with distance from a $M \sim 5$ earthquake.

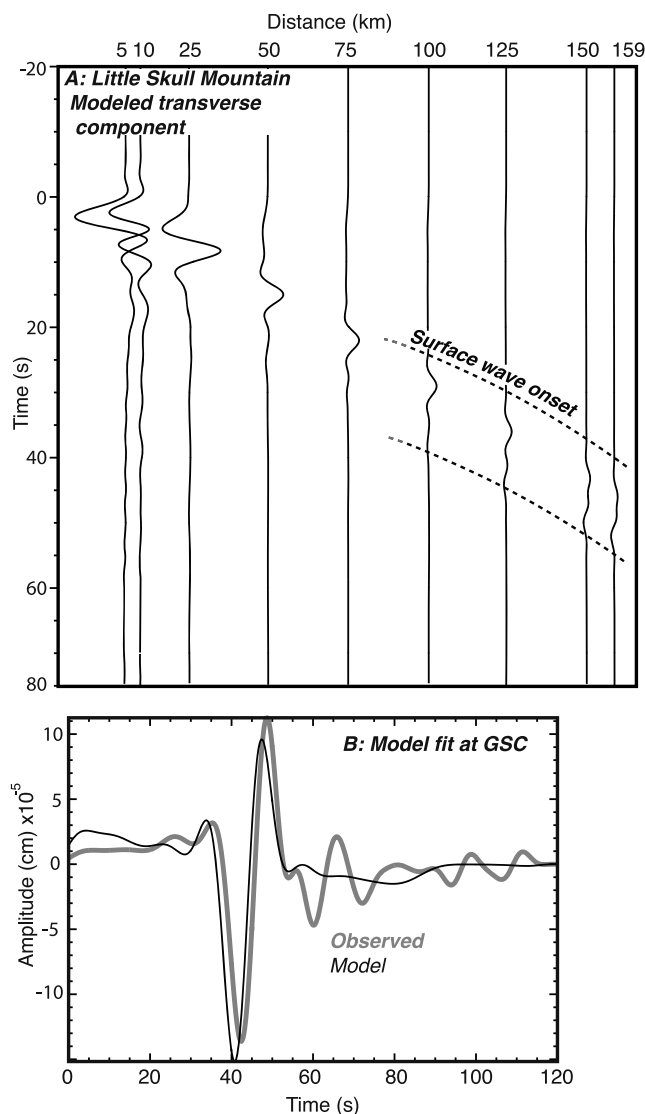


Figure 9. (a) Synthetic seismograms of transverse component versus source distance from the $M=5.7$ Little Skull Mountain earthquake. Dashed lines indicate amplitude onset of low-frequency (<0.2 Hz) surface waves. (b) Fit of modeled waveform to observed at station GSC (location shown in Figures 10 and 11).

(Figures 8 and 9). Therefore near-source dynamic triggering, if it occurs, is likely the result of direct or reflected P and/or S waves. Since the Little Skull Mountain earthquake was surrounded by aftershocks, while nearby nuclear explosions were not, we investigate differences in the spectra of primary phases from these two source types.

[30] Our hypothesis is that if near-source dynamic triggering occurs, then the phase or frequency band responsible may be lacking from explosion sources. To make the comparison, we analyze seismograms from regional stations for eight moderate earthquake, and eight nuclear sources (Figure 1 and Table 1). We download data from all broadband stations that lie within 5° of the Nevada Test Site from the Incorporated Research Institutes for Seismology (IRIS) Data Management Center, which include stations from the

Berkeley, Terrascope, Geoscope, and IRIS International Deployment of Accelerometers networks.

[31] Initial inspection of the seismograms shows generally on-scale, high-quality broadband data. We thus focus on analyzing data from the closest station, GSC, which recorded most of the earthquakes and explosions. Since the distances (200 to 270 km) and azimuths (9° to 22°) are similar to this station for these events, spectra amplitude differences should be the result of source differences, and not due to significant propagation differences. For earthquakes, differences in size and focal mechanism for each event result in spectral fluctuations; for explosions, source size and configuration also cause spectral differences.

[32] For spectra calculations, we group velocity windows for the Love (5.5 and 2.4 km/s) and Rayleigh (4.4 and 2.15 km/s) waves to isolate surface waves from other crustal arrivals. As described above, it appears that surface waves are unlikely triggers in the near-source region. We therefore wish to sample energy (crustal phases) that passes directly through the crust immediately surrounding the sources, like the aftershock zone of the Little Skull Mountain earthquake (Figure 10). Figure 11 shows relative spectra calculated and stacked for crustal phases and Rayleigh waves (for comparison) from eight earthquakes and five nuclear explosions recorded at station GSC. These are the same events used in the seismicity rate change analysis (Figure 1), where earthquake sources were shown to be much more likely to trigger other earthquakes. Nuclear sources were of comparable magnitudes (Table 1) but located ~ 60 km farther from GSC than the earthquakes, so we express amplitude spectra relative to peak amplitudes to enable direct comparison.

[33] We note that nuclear sources have slightly higher relative amplitude than earthquakes in the 0.5–1 Hz band, which is a commonly observed phenomenon of nuclear blasts, and represents overshoot caused by compaction of the source volume [e.g., *Mueller and Murphy, 1971; Aki et al., 1974*]. The spectral amplitude character of phases that arrive before surface waves is similar between nuclear and earthquake sources (Figure 11a), with peak amplitudes being equal, but with nuclear sources having lower amplitudes for parts of the band (0.1 to 0.03 Hz). We do not find significant differences between the seismogram components (Figures 11a and 11b), which is consistent with near-source recordings of large explosions that show “equipartitioning” between the seismic components (radial, transverse, vertical) for both chemical and nuclear sources [*Olsen and Peratt, 1994*] (Figure 12). The interpretation is that large explosions generate significant S waves, probably through growth of preexisting cracks [e.g., *Johnson and Sammis, 2001*] and collapse of, and wave mode conversion on cavity walls [e.g., *Liu and Ahrens, 2001*].

[34] The primary difference in earthquake and nuclear amplitude spectra we observe is that Rayleigh wave amplitudes are $\sim 50\%$ lower relative to peak in the nuclear sources in the sub-0.5-Hz range (Figure 11b). This result is the well-described body wave magnitude (m_b) versus surface wave (M_s) discriminant used to identify nuclear events at large distances and probably results from shallower nuclear source depths.

[35] To summarize our findings, surface waves with sufficiently low frequency to influence the crust where aftershocks are observed (Figure 7) following the Little Skull

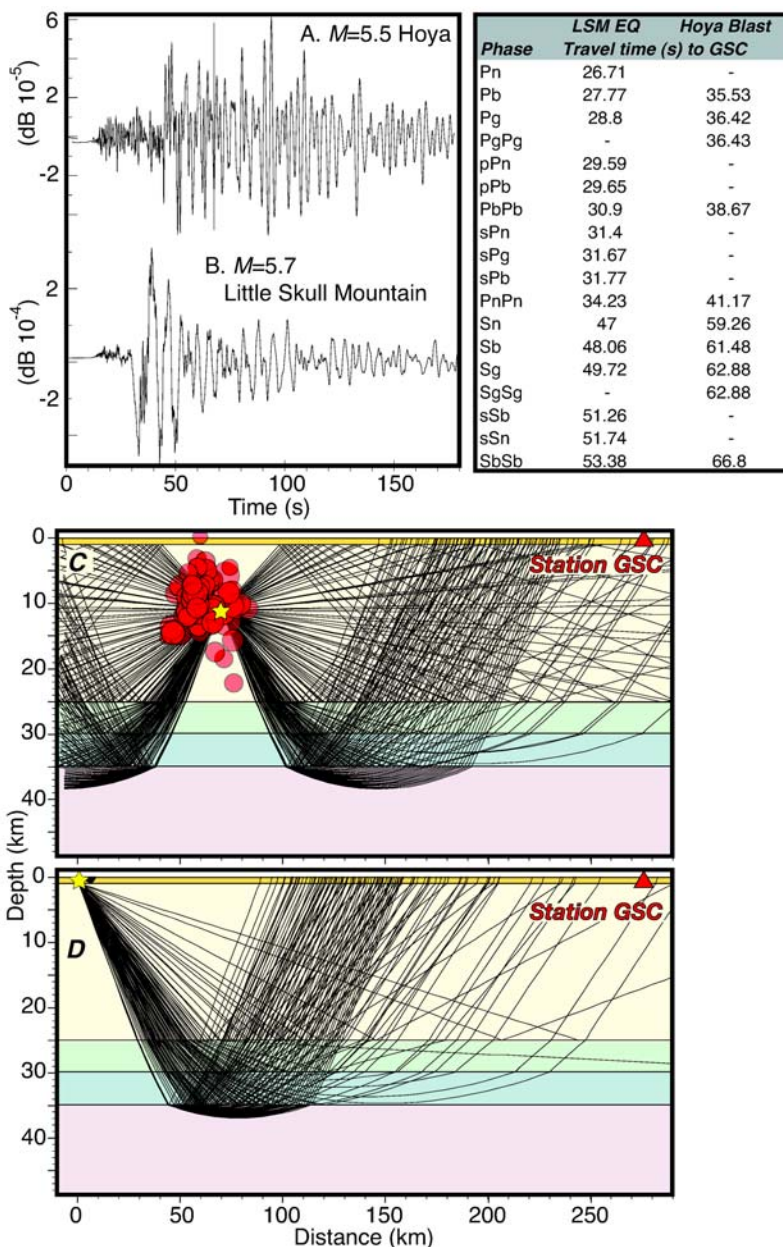


Figure 10. Transverse component seismograms from (a) the $M = 5.5$ “Hoya” nuclear explosion and (b) the $M = 5.7$ Little Skull Mountain earthquake (see Table 1 for source parameters). Zero time is set to the first P wave arrivals. The tabulation gives calculated expected arrival times relative to event origin times of presurface wave phases. (c) Ray trace through the velocity model of *Smith et al.* [2001] of crustal seismic waves that pass through the observed aftershock zone (first 24 h plotted) of the Little Skull Mountain earthquake. (d) Rays are plotted for crustal waves from the Hoya nuclear source; no aftershocks were recorded by ANSS networks despite the fact that direct P and S waves passed through a similar depth range as those from the Little Skull Mountain earthquake.

Mountain earthquake require ~ 75 – 80 km of offset to emerge (Figures 8 and 9). Thus waves that directly emit from sources are better candidates for near-source dynamic triggering. We compare spectral amplitudes of seismic phases from earthquake and nuclear sources that pass through near-source aftershock zones (Figure 10). We find that both source types impart similar dynamic stresses into the crust (Figure 11). Thus earthquake and nuclear sources appear

to deliver nearly the same dynamic stresses into the near-source crust, including S waves (Figures 11a, 11b, and 12).

5. Conclusions

[36] We reproduce the result that large explosions fail to trigger earthquakes, while comparable magnitude earthquakes do. Explosions generate small static stress changes

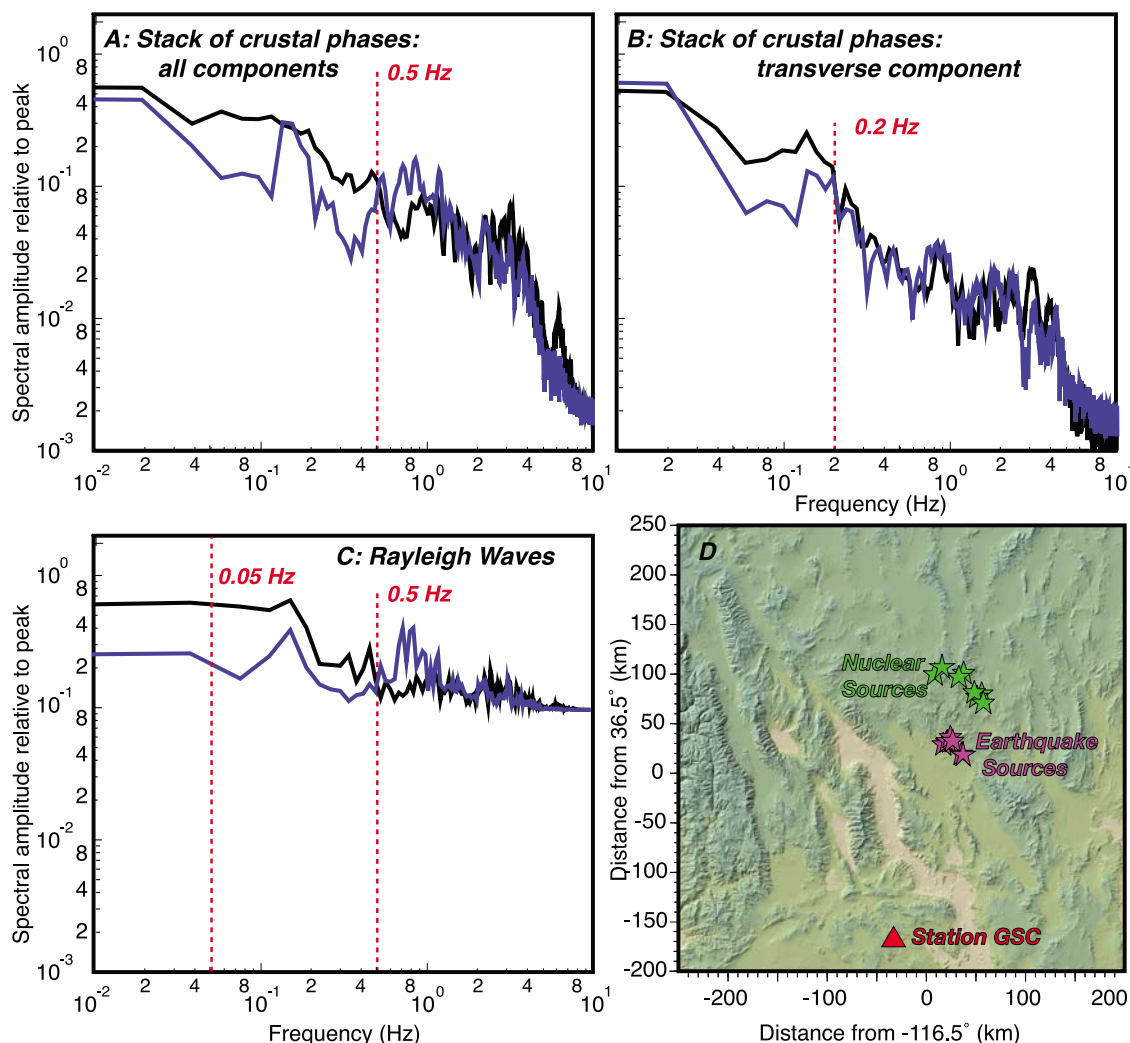


Figure 11. Comparison of amplitude spectra of stacked presurface wave arrivals: crustal phases from earthquakes (black trace) and nuclear explosions (blue trace) that pass through aftershock zones (Figure 10). Earthquakes and nuclear source spectral amplitudes were normalized to peak and stacked. (a) All components are combined. (b) Just the transverse component is shown. (c) Amplitudes of crustal phases are comparable across a broad frequency band, but Rayleigh waves from nuclear sources are much lower amplitude below 0.5 Hz than those from earthquakes. (d) Locations of earthquake (purple stars) and nuclear sources (green stars) and seismic station GSC, located ~ 200 to 270 km from the sources. These are the same events used in Figure 1, where earthquake sources were shown to be much more likely to trigger other earthquakes.

compared with earthquakes (Figure 4), so a simple explanation of the differences in near-source triggering is attribution of static stress change as the primary cause. Alternatively, differences in spectral amplitudes between earthquakes and nuclear sources that cause different dynamic stresses to be delivered into the crust might be the cause of the different triggering observations.

[37] Analysis of seismograms from explosion and earthquake sources reveals that explosions have half the amplitude relative to peak of low-frequency (≥ 0.5 Hz) surface waves than earthquakes. Long-period surface waves are associated with remote dynamic triggering [e.g., Hill, 2008; Velasco *et al.*, 2008] but have little amplitude in the near-source ($r \leq 50$ km) region where most aftershocks are observed [Karnik, 1962] (Figures 8 and 9), which is likely

a result of the distance necessary for surface wave energy to form out of a crustal waveguide [e.g., Savarensky *et al.*, 1970; Fu, 2006]. Thus, if dynamic triggering results only from low-frequency surface waves, it is unlikely to happen in the near-source region.

[38] We study the seismic phases that do pass from the sources directly into the near-source crust from comparable magnitude earthquakes and nuclear blasts. These phases were recorded on a broadband station (GSC; location shown in Figure 11) as presurface wave arrivals (Figure 10). Spectral amplitudes from earthquake and nuclear sources are similar across the frequency band, meaning that both source types deliver similar dynamic stresses into the near-source crust.

[39] We can readily explain aftershocks like those associated with the 1992 $M = 5.7$ Little Skull Mountain

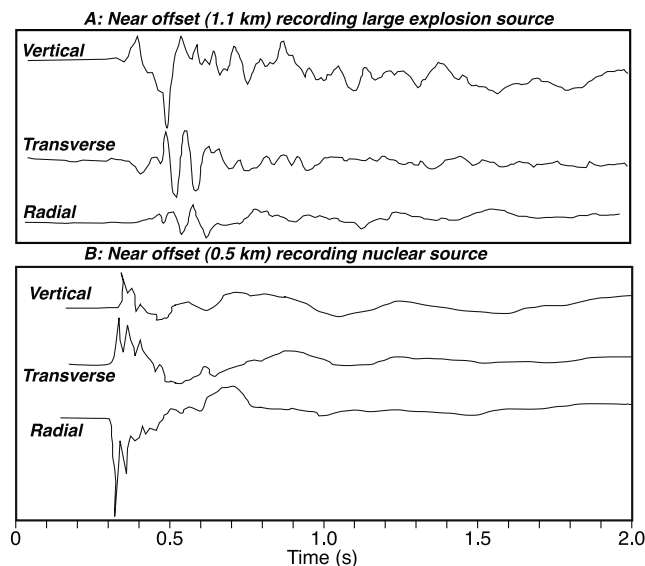


Figure 12. Near-source recordings of (a) a large ($M = 4.1$) chemical explosion and (b) a nuclear explosion ($M = 5.0$). Comparable amplitudes on all three components indicate that explosive sources are effective at generating primary S waves [Olsen and Peratt, 1994].

earthquake with a static stress change model (Figures 4 and 5). Given the dearth of aftershocks associated with nuclear blasts despite their ability to impart comparable dynamic stressing into the near-source crust as main shock earthquakes, we conclude that dynamic triggering plays little or no role in the near-source region where body waves dominate. Our observations are thus consistent with dynamic earthquake triggering being limited to a surface wave phenomenon.

[40] We suggest that dynamic triggering occurs at longer ranges because of one or more characteristics specific to surface waves: (1) surface waves have amplitude at longer periods than body waves [e.g., Stein and Wysession, 2003], (2) dispersion causes longer surface wave durations relative to near-source phases, and (3) surface waves propagate with a greater variety of polarization directions than body waves [e.g., Kulhánek, 2002], giving them a higher probability of aligning with fault planes of potentially triggered earthquakes.

[41] **Acknowledgments.** We thank Bill Walter at Lawrence Livermore National Laboratory for providing waveform data from Nevada Test Site blasts. We thank Jeanne Hardebeck and Joan Gomberg for comments on an earlier version of this paper. Thanks also to Associate Editor Rodolfo Console and two anonymous readers.

References

- Adushkin, V., and A. Spivak (1995), Aftershocks of underground nuclear explosion, in *Earthquakes Induced by Underground Nuclear Explosions: Environmental and Ecological Problems, NATO ASI Ser., Ser. 2*, vol. 4, edited by R. Console and A. Nikolaev, pp. 35–49, Springer, Berlin.
- Aki, K., and P. G. Richards (1980), *Quantitative Seismology: Theory and Methods*, W. H. Freeman, San Francisco, Calif.
- Aki, K., M. Bouchon, and P. Reasenberg (1974), Seismic source function for an underground nuclear explosion, *Bull. Seismol. Soc. Am.*, *64*, 131–148.
- Anderson, J. G., J. N. Brune, J. N. Louie, Y. Zeng, M. Savage, G. Yu, Q. Chen, and D. dePaolo (1994), Seismicity in the western Great Basin apparently triggered by the Landers, California, earthquake, 28 June 1992, *Bull. Seismol. Soc. Am.*, *84*, 863–891.

- Belardinelli, M. E., M. Cocco, O. Coutant, and F. Cotton (1999), Redistribution of dynamic stress during coseismic ruptures: Evidence for fault interaction and earthquake triggering, *J. Geophys. Res.*, *104*, 14,925–14,945, doi:10.1029/1999JB900094.
- Birch, F. (1966), Compressibility: Elastic constants, in *Handbook of Physical Constants*, edited by S. P. Clark Jr., *Mem. Geol. Soc. Am.*, *97*, 97–173.
- Boucher, G., A. Ryall, and A. E. Jones (1969), Earthquakes associated with underground nuclear explosions, *J. Geophys. Res.*, *74*, 3808–3820, doi:10.1029/JB074i015p03808.
- Brune, J. N., and P. W. Pomeroy (1963), Surface wave radiation patterns for underground nuclear explosions and small-magnitude earthquakes, *J. Geophys. Res.*, *68*, 5005–5028.
- Campillo, M., and R. J. Archuleta (1993), A rupture model for the 28 June 1992 Landers, California earthquake, *Geophys. Res. Lett.*, *20*, 647–650, doi:10.1029/92GL02822.
- Cotton, F., and O. Coutant (1997), Dynamic stress variations due to shear faults in a plane-layered medium, *Geophys. J. Int.*, *128*, 676–688, doi:10.1111/j.1365-246X.1997.tb05328.x.
- Das, S., and C. Scholz (1981), Off-fault aftershock clusters caused by shear stress increase?, *Bull. Seismol. Soc. Am.*, *71*, 1669–1675.
- Drellack, S. L., Jr., L. B. Prothro, and J. L. Gonzales (2001), A hydrostratigraphic model of the Pahute Mesa–Oasis Valley area, Nye County, Nevada, *Rep. DOE/NV/11718-646*, U. S. Dep. of Energy, Las Vegas, Nev.
- Felzer, K., and E. Brodsky (2005), Testing the stress shadow hypothesis, *J. Geophys. Res.*, *110*, B05S09, doi:10.1029/2004JB003277.
- Felzer, K. R., and E. E. Brodsky (2006), Decay of aftershock density with distance indicates triggering by dynamic stress, *Nature*, *441*, 735–738, doi:10.1038/nature04799.
- Felzer, K. R., R. E. Abercrombie, and G. Ekström (2003), Secondary aftershocks and their importance for aftershock forecasting, *Bull. Seismol. Soc. Am.*, *93*, 1433–1448, doi:10.1785/0120020229.
- Freed, A. M. (2005), Earthquake triggering by static, dynamic, and post-seismic stress transfer, *Annu. Rev. Earth Planet. Sci.*, *33*, 335–367, doi:10.1146/annurev.earth.33.092203.122505.
- Fu, L.-Y. (2006), Comparison of different one-way propagators for wave forward propagation in heterogeneous crustal wave guides, *Bull. Seismol. Soc. Am.*, *96*, 1091–1113, doi:10.1785/0120050159.
- Gomberg, J., and P. Bodin (1994), Triggering of the $M_s = 5.4$ Little Skull Mountain, Nevada, earthquake with dynamic strains, *Bull. Seismol. Soc. Am.*, *84*, 844–853.
- Gomberg, J., P. Bodin, and P. A. Reasenberg (2003), Observing earthquakes triggered in the near field by dynamic deformations, *Bull. Seismol. Soc. Am.*, *93*, 118–138, doi:10.1785/0120020075.
- Gomberg, J., P. Bodin, K. Larson, and H. Dragert (2004), Earthquake nucleation by transient deformations caused by the $M = 7.9$ Denali, Alaska, earthquake, *Nature*, *427*, 621–624, doi:10.1038/nature02335.
- Habermann, R. E. (1987), Man-made changes in seismicity rates, *Bull. Seismol. Soc. Am.*, *77*, 141–159.
- Hamilton, R. M., F. A. McKeown, and J. H. Healy (1969), Seismic activity and faulting associated with a large underground explosion, *Science*, *166*, 601–604, doi:10.1126/science.166.3905.601.
- Hardebeck, J. L., J. J. Nazareth, and E. Hauksson (1998), The static stress change triggering model: Constraints from two southern California earthquake sequences, *J. Geophys. Res.*, *103*, 24,427–24,437, doi:10.1029/98JB00573.
- Harris, R. A. (1998), Introduction to special section: Stress triggers, stress shadows, and implications for seismic hazard, *J. Geophys. Res.*, *103*, 24,347–24,358, doi:10.1029/98JB01576.
- Harris, R. A., and R. W. Simpson (1996), In the shadow of 1857: The effect of the great Ft. Tejon earthquake on subsequent earthquakes in southern California, *Geophys. Res. Lett.*, *23*, 229–232, doi:10.1029/96GL00015.
- Herrmann, R. B., and J. C. Ammon (2002), *Computer Programs in Seismology*, Saint Louis Univ., Saint Louis, Mo.
- Hill, D. P. (2008), Dynamic stresses, Coulomb failure, and remote triggering, *Bull. Seismol. Soc. Am.*, *98*, 66–92, doi:10.1785/0120070049.
- Hill, D. P., et al. (1993), Seismicity in the western United States remotely triggered by the $M 7.4$ Landers, California, earthquake of June 28, 1992, *Science*, *260*, 1617–1623, doi:10.1126/science.260.5114.1617.
- Houser, F. N. (1969), Subsidence related to underground nuclear explosions, Nevada Test Site, *Bull. Seismol. Soc. Am.*, *59*, 2231–2251.
- Johnson, L. R., and C. G. Sammis (2001), Effects of rock damage on seismic waves generated by explosions, *Pure Appl. Geophys.*, *158*, 1869–1908, doi:10.1007/PL00001136.
- Kagan, Y. Y. (2004), Short-term properties of earthquake catalogs and models of earthquake source, *Bull. Seismol. Soc. Am.*, *94*, 1207–1228, doi:10.1785/012003098.
- Karnik, V. (1962), Amplitude-distance curves of surface waves at short epicentral distances ($A < 2000$) km, *Stud. Geophys. Geod.*, *6*, 340–346, doi:10.1007/BF02585233.

- Kennett, B. L. (1983), *Seismic Wave Propagation in Stratified Media*, 342 pp., Cambridge Univ. Press, Cambridge, U. K.
- Kilb, D., J. S. Gombert, and P. Bodin (2000), Triggering of earthquake aftershocks by dynamic stresses, *Nature*, *408*, 570–574, doi:10.1038/35046046.
- Kilb, D., J. Gombert, and P. Bodin (2002), Aftershock triggering by complete Coulomb stress changes, *J. Geophys. Res.*, *107*(B4), 2060, doi:10.1029/2001JB000202.
- King, G. C. P., R. S. Stein, and J. Lin (1994), Static stress changes and the triggering of earthquakes, *Bull. Seismol. Soc. Am.*, *84*, 935–953.
- Kulhánek, O. (2002), The structure and interpretation of seismograms, in *International Handbook of Earthquake and Engineering Seismology, Int. Geophys. Ser.*, vol. 81, edited by W. H. K. Lee et al., pp. 333–348, Academic, Amsterdam.
- Liu, C., and T. J. Ahrens (2001), Wave generation from explosions in rock cavities, *Pure Appl. Geophys.*, *158*, 1909–1949, doi:10.1007/PL0001137.
- Lohman, R. B., M. Simons, and B. Savage (2002), Location and mechanism of the Little Skull Mountain earthquake as constrained by satellite radar interferometry and seismic waveform modeling, *J. Geophys. Res.*, *107*(B6), 2118, doi:10.1029/2001JB000627.
- Mallman, E. P., and T. Parsons (2008), A global search for stress shadows, *J. Geophys. Res.*, *113*, B12304, doi:10.1029/2007JB005336.
- Marsan, D., and S. S. Nalbant (2005), Methods for measuring seismicity rate changes: A review and a study of how the M_w 7.3 Landers earthquake affected the aftershock sequence of the M_w 6.1 Joshua Tree earthquake, *Pure Appl. Geophys.*, *162*, 1151–1185, doi:10.1007/s00024-004-2665-4.
- Matthews, M. V., and P. A. Reasenberg (1988), Statistical methods for investigating quiescence and other temporal seismicity patterns, *Pure Appl. Geophys.*, *126*, 357–372, doi:10.1007/BF00879003.
- Meremonte, M., J. Gombert, and E. Cranswick (1995), Constraints on the 29 June 1992 Little Skull Mountain, Nevada, earthquake sequence provided by robust hypocenter estimates, *Bull. Seismol. Soc. Am.*, *85*, 1039–1049.
- Mueller, R. A., and J. R. Murphy (1971), Seismic characteristics of underground nuclear detonations. Part I. Seismic spectrum scaling, *Bull. Seismol. Soc. Am.*, *61*, 1675–1692.
- Nikolaev, A. (1995), Inducing of earthquakes by underground nuclear explosions, in *Earthquakes Induced by Underground Nuclear Explosions: Environmental and Ecological Problems, NATO ASI Ser., Ser. 2*, vol. 4, edited by R. Console and A. Nikolaev, pp. 11–19, Springer, Berlin.
- Olsen, K. H., and A. L. Peratt (1994), Free-field ground motions for the nonproliferation experiment: Preliminary comparisons with nearby nuclear events, in *Proceedings of the Symposium on the Non-proliferation Experiment: Results and Implications for Test Ban Treaties, Rep. CONF-9404100*, edited by M. D. Denny, Lawrence Livermore Natl. Lab., Livermore, Calif.
- Randall, G. R., C. J. Ammon, and T. J. Owens (1995), Moment tensor estimation using regional seismograms from a Tibetan Plateau portable network deployment, *Geophys. Res. Lett.*, *22*, 1665–1668, doi:10.1029/95GL00909.
- Reasenberg, P. A., and R. W. Simpson (1992), Response of regional seismicity to the static stress change produced by the Loma Prieta earthquake, *Science*, *255*, 1687–1690, doi:10.1126/science.255.5052.1687.
- Richards, P. G., and G. Ekström (1995), Earthquake activity associated with underground nuclear explosions, in *Earthquakes Induced by Underground Nuclear Explosions: Environmental and Ecological Problems, NATO ASI Ser., Ser. 2*, vol. 4, edited by R. Console and A. Nikolaev, pp. 21–34, Springer, Berlin.
- Savarensky, E. F., S. A. Fedorov, and O. E. Starovojt (1970), On surface seismic waves formation, *Pure Appl. Geophys.*, *82*, 66–84, doi:10.1007/BF00876170.
- Schultz, A., and Q. Li (1995), Uniaxial strength testing of non-welded Calico Hills tuff, Yucca Mountain, Nevada, *Eng. Geol. Amsterdam*, *40*, 287–299, doi:10.1016/0013-7952(95)00041-0.
- Smith, K. D., J. N. Brune, D. dePolo, M. K. Savage, R. Anooshehpour, and A. F. Sheehan (2001), The 1992 Little Skull Mountain earthquake sequence, southern Nevada test site, *Bull. Seismol. Soc. Am.*, *91*, 1595–1606, doi:10.1785/0120000089.
- Stein, R. S. (1999), The role of stress transfer in earthquake occurrence, *Nature*, *402*, 605–609, doi:10.1038/45144.
- Stein, R. S., and M. Lisowski (1983), The 1979 Homestead Valley earthquake sequence, California: Control of aftershocks and postseismic deformation, *J. Geophys. Res.*, *88*, 6477–6490, doi:10.1029/JB088iB08p06477.
- Stein, S., and M. Wyssession (2003), *An Introduction to Seismology, Earthquakes, and Earth Structure*, 498 pp., Blackwell, Malden, Mass.
- Stevens, J., and S. Day (1985), The physical basis of m_b , M_s , and variable frequency magnitude methods for earthquake/explosion discrimination, *J. Geophys. Res.*, *90*, 3009–3020, doi:10.1029/JB090iB04p03009.
- Toda, S., and R. S. Stein (2003), Toggling of seismicity by the 1997 Kagoshima earthquake couplet: A demonstration of time-dependent stress transfer, *J. Geophys. Res.*, *108*(B12), 2567, doi:10.1029/2003JB002527.
- Toksoz, M. N., and H. H. Kehler (1972), Tectonic strain-release characteristics of CANNIKIN, *Bull. Seismol. Soc. Am.*, *62*, 1425–1438.
- Velasco, A. A., S. Hernandez, T. Parsons, and K. Pankow (2008), The ubiquitous nature of dynamic triggering, *Nat. Geosci.*, *1*, 375–379, doi:10.1038/ngeo204.
- Voisin, C., F. Cotton, and S. Di Carli (2004), A unified model for dynamic and static stress triggering of aftershocks, antishocks, remote seismicity, creep events, and multisegmented rupture, *J. Geophys. Res.*, *109*, B06304, doi:10.1029/2003JB002886.
- Walter, W. R. (1993), Source parameters of the June 29, 1992 Little Skull Mountain earthquake from complete regional waveforms at a single station, *Geophys. Res. Lett.*, *20*, 403–406, doi:10.1029/92GL03031.
- Walter, W. R., K. M. Mayeda, and H. J. Patton (1995), Phase and spectral ratio discrimination between NTS earthquakes and explosions. Part I: Empirical observations, *Bull. Seismol. Soc. Am.*, *85*, 1050–1067.
- Wiemer, S., and M. Wyss (2002), Mapping spatial variability of the frequency-magnitude distribution of earthquakes, *Adv. Geophys.*, *45*, 259–302.
- Woessner, J., and S. Wiemer (2005), Assessing the quality of earthquake catalogues: Estimating the magnitude of completeness and its uncertainty, *Bull. Seismol. Soc. Am.*, *95*, 684–698, doi:10.1785/0120040007.
- Working Group on California Earthquake Probabilities (2003), Earthquake probabilities in the San Francisco Bay region: 2002 to 2031, *U.S. Geol. Surv. Open File Rep.*, *03-214*.
- Yamashina, K. (1978), Induced earthquakes in the Izu Peninsula by the Izu-Hanto-Oki earthquake of 1974, Japan, *Tectonophysics*, *51*, 139–154, doi:10.1016/0040-1951(78)90237-8.
- Ziv, A. (2006), What controls the spatial distribution of remote aftershocks?, *Bull. Seismol. Soc. Am.*, *96*, 2231–2241, doi:10.1785/0120060087.
- Ziv, A., and A. M. Rubin (2003), Implications of rate-and-state friction for properties of aftershock sequence: Quasi-static inherently discrete simulations, *J. Geophys. Res.*, *108*(B1), 2051, doi:10.1029/2001JB001219.

T. Parsons, U.S. Geological Survey, 345 Middlefield Road, MS 999, Menlo Park, CA 94025, USA. (tparsons@usgs.gov)
 A. A. Velasco, Department of Geological Sciences, University of Texas at El Paso, El Paso, TX 79968-0555, USA.